A Catalytic and Selective Scissoring Molecular Tool for Quadruplex Nucleic Acids

Matteo Nadai,[†,‖] Filippo Doria,[‡,‖] Matteo Scalabrin,[†] Valentina Pirota,[‡] Vincenzo Grande,[‡] Greta Bergamaschi,[‡] Valeria Amendola,[‡] Fernaldo Richtia Winnerdy,[§] Anh Tuân Phan,[§] Sara N. Richter,*[†] and Mauro Freccero*[‡]

[†]Department of Molecular Medicine, University of Padua, via Gabelli 63, 35121 Padua, Italy
[‡]Department of Chemistry, University of Pavia, V. le Taramelli 10, 27100 Pavia, Italy
[§]School of Physical and Mathematical Sciences, Nanyang Technological University, Singapore 637371, Singapore

Ⓢ *Supporting Information*

ABSTRACT: A copper complex embedded in the structure of a water-soluble naphthalene diimide has been designed to bind and cleave G-quadruplex DNA. We describe the properties of this ligand, including its catalytic activity in the generation of ROS. FRET melting, CD, NMR, gel sequencing, and mass spectrometry experiments highlight a unique and unexpected selectivity in cleaving G-quadruplex sequences. This selectivity relies both on the binding affinity and structural features of the targeted G-quadruplexes.

Nucleic acid sequences rich in guanine (G) base are able to fold into G-quadruplex (G4) structures in the presence of suitable alkali metals (K⁺ or Na⁺). G4s are characterized by square-planar configurations of four Gs, arranged through Hoogsteen hydrogen bonding, and they differ from each other by chain number and orientation.[1−3] These supramolecular structures have received increasing attention as they are involved in genomic instability,[1,4] telomerase dysfunction,[5,6] regulation of gene expression,[7,8] and viral transcription.[9,10] In particular, these structures have been shown to have regulatory functions for telomere extension and maintenance,[11] thus playing important roles in cancer biology.[12−14] In addition, G4s involved in the life cycle of different viruses, such as HIV-1,[15−18] HSV-1,[19] EBV,[20,21] HCV, and others,[22] have been reported. Consequently, small molecules that target, stabilize, and also modify G4s represent potential anticancer agents[23,24] and antiviral drugs.[25,26] To date, a large number of G4 ligands, including naphthalene diimides (NDIs), have been published, but the selective cleavage of G4s has only been achieved once, on intramolecular telomeric G4s.[27] Thus, far, none of the investigated DNA-cleavers can target nontelomeric G4s, nor any selective scissoring, discriminating a G4 among others, has been reported yet. Among the transition metals that participate in various metabolic processes in living organisms, copper is one of the essential enzyme cofactors owing to its redox properties. This has inspired a catalytic metallo-drug strategy in nucleic acid chemistry.[27] In fact, Cu ligands were found to be active in vitro[28] and in vivo via metal-mediated DNA cleavage through reactive oxygen species (ROS).[7,27,29−32] In our previous study,

we developed core-substituted NDIs able to coordinate with low affinity (K_{-d} = 2.0 × 10⁵ M⁻¹) Cu(II) in close proximity to the aromatic core.[33] Much higher affinity (K_{-d} > 10¹⁶ M⁻¹) is required to generate ROS in the presence of nucleic acids to avoid Cu(II) translocation. In this study, we merged both the Cu and G4 binding features in a NDI−Cu complex, containing a diethylenetriamine (DETA) substituent (**NDI−Cu−DETA**, Figure 1), which effectively and selectively chelates Cu²⁺ at
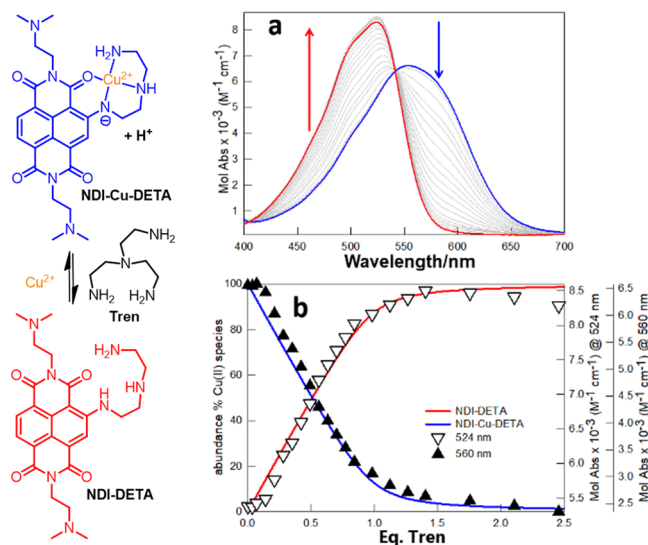

Figure 1. Structures and **NDI-Cu-DETA** (50 μM) titration by **Tren**: (a) absorption spectra and (b) distribution diagram.

physiological pH (Figure S1−S3, Table S1). The high-affinity constant for Cu²⁺(K_{-d} = 1.99 × 10¹⁷ M⁻¹) has been measured by titration with **Tren** as competing ligand (Figure S4−S6).[34]

Substituted NDIs are well-known reversible ligands, binding G4s by end-stacking interactions with high affinity.[35−38] To determine whether the addition of the Cu moiety affected G4-selectivity, **NDI-Cu-DETA** and its NDI Cu-free precursor (**NDI−DETA**) were tested on both cellular and viral G4 oligonucleotides and dsDNA (Table S2) by FRET melting
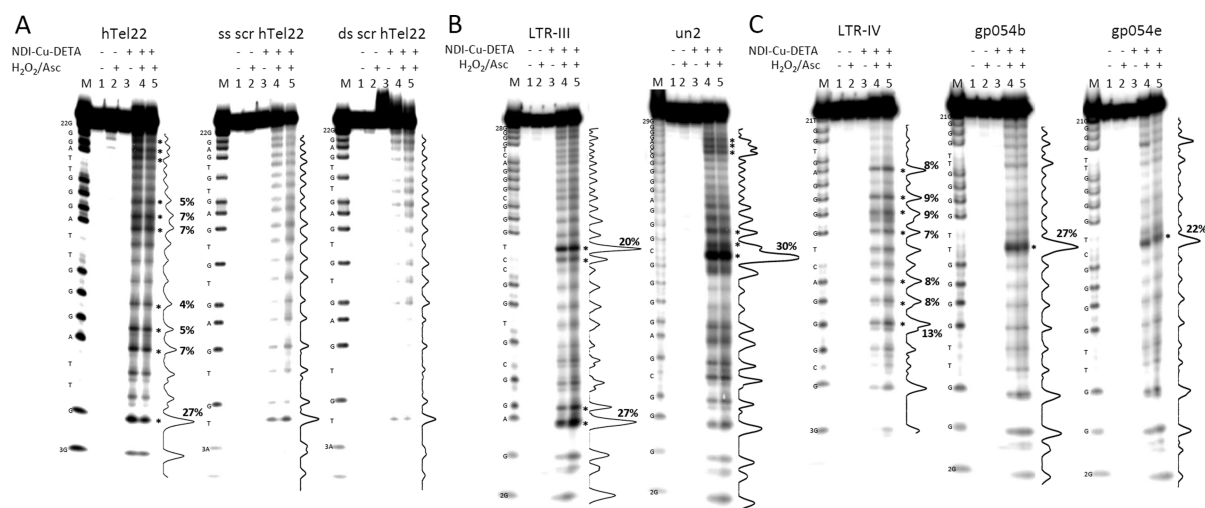
Figure 2. NDI−Cu−DETA-induced cleavage of G4-folded sequences: (A) G4-folded telomeric sequence (hTel22), a scrambled sequence unable to fold into G4 (ss scr hTel22, same base composition and different sequence) and its dsDNA (ds scr hTel22, Table S2); (B) LTR-III and un2; (C) LTR-IV, gp054b and gp054e. Oligonucleotides (0.25 μM) reacted with NDI−Cu−DETA (A) 25 μM, (B and C) 3.12 μM) for 2.5 or 5 min (lanes 4 and 5, respectively) in the presence of 1 mM sodium ascorbate and 1 mM hydrogen peroxide, as indicated. Samples were run on denaturing polyacrylamide gels. Asterisks highlight major cleavage sites, M = marker lane. Panels include intensity profiles of lanes 4 and quantification of the major bands (%).

studies at different K⁺ concentrations (Table S3 and Figure S23A). While the introduction of Cu slightly destabilized the G4s (ΔT_m on average 18% lower than with NDI−DETA), NDI−Cu−DETA retained G4 selectivity. ΔT_m were inversely dependent on the stability of the G4 oligonucleotide itself (ΔT_m increased at lower K⁺ concentration and was not measurable in c-myc and bcl-2, which displayed the highest intrinsic T_m). G4/NDI−Cu−DETA complex stability was also assessed by thermal denaturation analysis monitored by CD (Figure S23B). To give a meaningful comparison, the K⁺ amount was modulated so that initial T_m values of all tested G4s were maintained in the 50−60 °C range (Table S4). ΔT_m values above 22 °C were observed for mammalian hTel22, c-myc, bcl-2, and c-kit2 and for HIV-1 LTR-III+IV and LTR-IV and HSV-1 gp054b (Table S4). No conformation dependence was noted. Under physiological conditions (50 mM phosphate buffer pH 7.4), NDI−Cu−DETA exhibited catalytic activity for ROS generation, causing the oxidation of an external substrate such as 4-tertbutylcatechol (Figure S7). To mimic the reducing intracellular environment, as a useful model reaction for ROS generation, we took advantage of the Cu(I)-catalyzed reduction of hydrogen peroxide in the presence of ascorbate, which yields hydroxyl radicals.[39] To confirm the involvement of diffusible hydroxyl radicals under the catalytic conditions used, we monitored at 440 nm, in 50 mM phosphate buffer (pH 7.4, 37 °C; Figure S8), the effective bleaching of p-nitrosodimethylaniline (p-NDA).[40,41] Ligand interaction with G4s drove the reactivity onto the DNA, making its oxidation a competitive process with the p-NDA and erasing its bleaching (Figure S8).

NDI−Cu−DETA was evaluated as a specific G4 DNA cleaver in the presence of ascorbic acid and hydrogen peroxide for 2.5−5 min at 25 °C. The complex was initially reacted with a G4-folded telomeric sequence (i.e., hTel22), a scrambled sequence unable to fold into G4 (ss scr hTel22) and its dsDNA (ds scr hTel22, Table S2). The resulting reaction mixtures were analyzed by denaturing polyacrylamide gel electrophoresis. Major cleavage sites were observed in the

presence of NDI−Cu−DETA on hTel22 at bases G4, A7−G9, A13−G15, and A19−G21 (Figure 2A). In contrast, much weaker and unspecific cleavage sites were present in the control mutant ss and dsDNAs. Cleavage reactivity of NDI−Cu−DETA was next investigated on a panel of structurally and topologically different G4s, i.e., LTR-III and LTR-IV found in HIV-1, un2, gp054b, and gp054e found in HSV-1, c-myc, bcl-2, c-kit1, and c-kit2 found in mammals (Table S2). The cleavage efficiency, compared to the cleavage of the least reactive ds scr hTel22, was 1.7 and 2.5 higher for ss scr hTel22 and hTel, respectively. All other G4s were cleaved at even higher folds: 4x c-myc and bcl-2, 6× LTR-IV, 7.3× c-kit1, 7.4× gp054b, 7.7× gp054e, 8.2× LTR-III, 9.5× un2, and 12.8 c-kit2 (Table S5).

Selectivity for single sites was considered when cleavage bands corresponded to at least 20% of total cleavage. Site selectivity was obtained on HIV-1 LTR-III (A4 27% and T14 20%), HSV-1 un2 (C13−-G15 30%) (Figure 2B), gp054b and gp054e (T11 27% and C11 22%) (Figure 2C). In contrast, LTR-IV (Figure 2C), c-myc and bcl-2 (Figure S11A), and c-kit1 and c-kit2 (Figure S11B) revealed multisite reactivity (Table S5). Very interestingly, the two HSV-1 sequences gp054b and gp054e, which differ by only one nucleotide in two loops (Table S2), exhibited the exact same reactivity on the one different nucleotide in one of the loops (Figure 2C). Also in the case of these G4-folded oligonucleotides, cleavage was more efficient and site-selective toward the G4s vs mutated ss and dsDNAs derived from the tested oligonucleotides (Figure S9 and Table S2). To further confirm G4 selectivity, excess of the mutated dsDNAs was used in a competition cleavage assay in the presence of NDI−Cu−DETA (Figure S10). The ds competitors did not significantly alter the cleavage of the corresponding G4 oligonucleotides when used at 2-fold excess: the relative cleavage was reduced by 12% in LTR-III and 4% in un2 and was not reduced in gp054b. Only at 4-folds, the competitors inhibited site-selective cleavage on the G4s. G4 site-selectivity may be the result of NDI−Cu−DETA-mediated "on-target" hydroxyl radical generation compared to in

solution radical generation in the case of the unfolded ss and ds oligonucleotides. This hypothesis is corroborated by cleavage data reported for a copper–peptide complex conjugated to acridine, where the ligand exhibited preferred binding to hTel22 G4 over duplex DNA.[27] This data also suggests a structure- rather than sequence-dependent selectivity by the **NDI−Cu−DETA**, which remains stable under the oxidative conditions of the DNA cleavage studies (Figures S12 and S13).

To assess the extension of **NDI−Cu−DETA** reactivity toward DNA bases, LTR-III G4 was treated with hot piperidine, which stimulates phosphodiester bond cleavage at reacted bases (Figure S14). Piperidine increased band intensity both at the main sites of **NDI−Cu−DETA**-induced cleavage and at other sites (∗ and §, respectively, in Figure S14), indicating that base damage without cleavage occurred to a lesser extent at other bases too. At longer reaction times, **NDI−Cu−DETA** was able to induce cleavage also in the absence of H_2O_2 (Figure S15), suggesting the possibility of exploiting this reaction without oxidative stress. Mannitol, a specific hydroxyl radical scavenger,[42] did not affect the **NDI−Cu−DETA**-induced cleavage (Figure S15) in the presence of G4s. This evidence indicates site-specific generation of the hydroxyl radical without effective off-target diffusion.

To clarify the cleavage mechanism, one of the most intense cleavage sites in LTR-III G4 (C13 + T14 bands) was excised from the polyacrylamide gel and analyzed by MS (Figure 3).
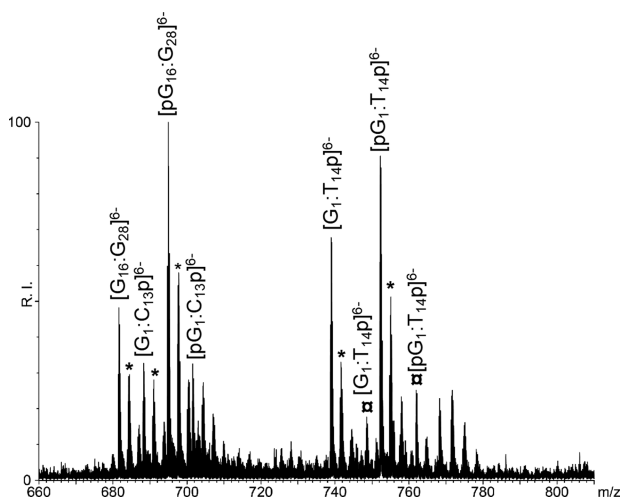

Figure 3. Spectra of the 5′-phosphate LTR-III cleavage band at C13 + T14 extracted and analyzed by ESI-MS. The symbol ∗ represents the oxidized peaks (exp. mass shift 15.99 amu). The symbol ¤ represents the cleavage products with 3′-phosphoglycolate modification (exptl mass shift 57.99 amu). All peaks are labeled with the matching sequence having the highest MS/MS coverage.

MS and MS/MS characterization[43] of the products indicated the presence of several fragments of similar mass, i.e., pG1:C13p, pG1:T14p, pC13:G28p, pT14:G28p), which showed that **NDI−Cu−DETA** cut LTR-III predominantly at the 3′ side of T14 and to a lesser extent C13 (Figure S16). Detection of pG1:T14p (3′-phosphate and 3′-phosphoglycolate) and pG16:G28 (5′-phosphate) products indicated reactivity of **NDI−Cu−DETA** at H1′ and H4′ of the ribose moiety with consequent cleavage of the phosphate backbone, degradation of G15 and release of pG1:T14p and pG16:G28.[44,45] In addition, oxidized G4s and guanosine monophosphates (Figures S17 and S18, respectively) were

detected by MS upon S1 nuclease digestion. The presence of oxidized bases in the absence of abasic cleavage products (Figure 3) suggests that base oxidation is not the main mechanism of DNA cleavage. These data are in line with the additional cleavage at oxidized bases observed upon treatment with piperidine (Figure S14). Therefore, H1′ and H4′ abstractions by the hydroxyl radical represent the main mechanism of the G4 cleavage, in agreement with previously reported mechanism of cleavage.[27] To test if cleavage specificity paralleled the affinity of **NDI−Cu−DETA** toward G4 oligonucleotides, binding affinity was assessed by MS.

Oligonucleotides showing both site-specific (LTR-III, un2, gp054b, gp054e) and multisite (LTR-IV, hTel22) cleavage were considered. In a 1:1 complex stoichiometry, the highest affinity was observed for LTR-III, followed by un2. LTR-IV and hTel22 showed intermediate affinity, while the two HSV-1 G4s (gp054b and gp054e) were bound with the lowest efficiency (Figure S19 and Table S6). These data suggest that fraction-bound%[46] is one of the driving forces toward site-specific cleavage. However, other structural features, as in the case of gp054b and gp054e, may control the cleavage site.

The nature of the **NDI−Cu−DETA** complexes with c-myc, c-kit1, and LTR-III was investigated by one-dimensional ^{1}H NMR titration. Ligand binding to the G4 structures should affect the signals of DNA protons near the binding site. In fact, for LTR-III, broadening upon addition of the compound was observed for the peaks of the duplex stem (G5 and G6) and one of the guanine in the top tetrad (G26) (Figure 4).[47] These
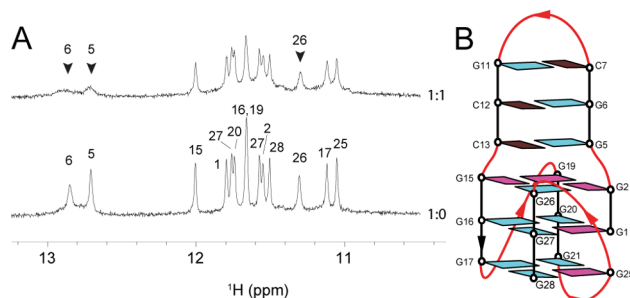

Figure 4. (A) ^{1}H NMR spectra of LTR-III (100 μM), free and bound to **NDI−Cu−DETA** at 1:1 ratio. The black arrows indicate imino protons of G5, G6 from the duplex and G26 from the top tetrad, which are preferentially broadened upon addition of the compound. Buffer conditions: 70 mM KCl, 20 mM phosphate buffer, pH 7.0. (B) Schematic of LTR-III G-quadruplex fold, cyan, magenta, and brown indicate *anti*-guanine, *syn*-guanine, and cytosine residues, respectively.

data indicate a preference of the ligand to bind LTR-III at the duplex−quadruplex junction. For c-myc and c-kit1 G4s, the imino protons of the 5′-end G-tetrad were broadened first, followed by those of other guanines, indicating the preferential binding of the compound at the 5′-end G-tetrad (Figure S20). The preferred binding sites of the compound are consistent with the major cutting sites observed by gel in both LTR-III and c-myc (Figure 2B and Figure S11A, respectively). For c-kit1, the cleavage data (Figure S11B) could be explained by a coexistence of both the preferred biding site at the 5′-end G-tetrad and an additional binding site near the bottom tetrad or/and coexistence of an additional conformation (caption of Figure S20).

To further support that site-specific generation of the hydroxyl radical by **NDI−Cu−DETA** is the controlling factor

of the cleavage selectivity, we performed **NDI−Cu−DETA** docking binding analysis on the LTR-III G4, whose structure in solution has been elucidated by NMR studies.[47] Docking scoring analysis was performed in end-stacking and groove-binding modes (Figure 5), with −9.3 and −8.5 kcal/mol
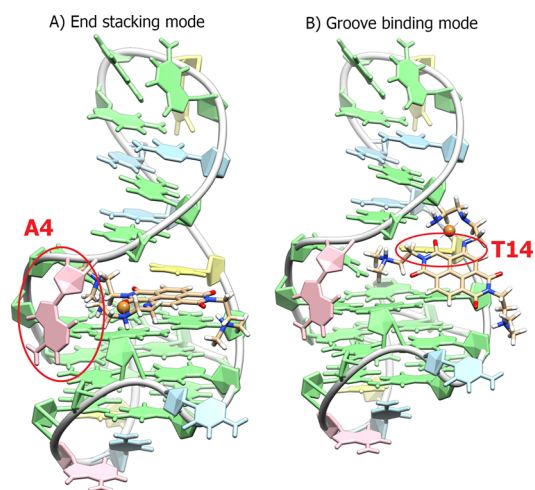

Figure 5. Side views of the binding modes with highest affinity predicted by molecular docking of **NDI−Cu−DETA** to LTR-III-G4 (A, pink; C, blue; G, green; T, yellow). Score function: (A) −9.3 kcal mol^{-1}; (B) −8.5 kcal mol^{-1}. Red circles highlight major cleavage sites in close proximity to the Cu(II) binding cavity.

affinity, respectively. In the end-stacking mode, **NDI−Cu−DETA** binds only one end of the hybrid-G4 (Figure 5A), placing the Cu binding cavity very close to the deoxyribose moieties at both A4 and G5.

On the contrary, in the groove-binding mode, **NDI−Cu−DETA** binds the LTR-III G4 (Figure 5B), placing the Cu binding cavity nearby the deoxyribose moieties at C13 and T14. The docking data are remarkably consistent with the results of the above induced cleavage experiments (Figure 2B). Both NMR-titration and docking data imply that the site-preferred scission in LTR-III G4 by **NDI−Cu−DETA** vs c-myc and c-kit1 G4s has to be ascribed to the extra-affinity conferred by the junction environment, as also suggested by the MS affinity data.

In conclusion, we have designed a novel naphthalene diimide Cu(II) complex acting as G4-cleaving agent, which targets selected G4 structures among others, with unexpected site selectivity. Our new **NDI−Cu−DETA** is stable when bound to a G4, producing hydroxyl radicals both in the presence and absence of H_2O_2. In contrast to previously published non site-selective cleavers,[27] hydroxyl radicals are produced in close proximity to the Cu coordination sphere: in the case of HIV-1 LTR-III-G4 and other definite G4s, such as un2 and gp054 found in HSV-1, hydroxyl radicals react on the target, without diffusing in solution (Figure S8). The observed site-selectivity relies on the **NDI−Cu−DETA**:G4 binding geometry, which defines the proximity of the Cu catalytic site to nearby regions (i.e., loops), independently of the target sequence. Our compound represents the first step toward the development of efficient cleavers for distinct G4s, to be used as valuable tools for elucidating G4 formation and resolution. Further improvement in their G4 vs dsDNA selectivity will be sought for in vivo application, such as for the treatment of G4-related diseases.

ASSOCIATED CONTENT

Supporting Information

The Supporting Information is available free of charge on the ACS Publications website at DOI: 10.1021/jacs.8b05337.

Experimental details, materials, synthesis and characterization of **NDI-Cu-DETA**, oligonucleotides, biophysical assays, and MS analysis (PDF)

AUTHOR INFORMATION

Corresponding Authors
*mauro.freccero@unipv.it
*sara.richter@unipd.it

ORCID
Valeria Amendola: 0000-0001-5219-6074
Anh Tuân Phan: 0000-0002-4970-3861
Sara N. Richter: 0000-0002-5446-9029
Mauro Freccero: 0000-0002-7438-1526

Author Contributions
‖M.N. and F.D. contributed equally.

Notes
The authors declare no competing financial interest.

REFERENCES

(1) Lopes, J.; Piazza, A.; Bermejo, R.; Kriegsman, B.; Colosio, A.; Teulade-Fichou, M. P.; Foiani, M.; Nicolas, A. *EMBO J.* **2011**, *30*, 4033−46.
(2) Davis, J. T. *Angew. Chem., Int. Ed.* **2004**, *43*, 668−98.
(3) Islam, M. M.; Fujii, S.; Sato, S.; Okauchi, T.; Takenaka, S. *Molecules* **2015**, *20*, 10963−79.
(4) Bedrat, A.; Lacroix, L.; Mergny, J. L. *Nucleic Acids Res.* **2016**, *44*, 1746−59.
(5) Fouquerel, E.; Lormand, J.; Bose, A.; Lee, H.-T.; Kim, G. S.; Li, J.; Sobol, R. W.; Freudenthal, B. D.; Myong, S.; Opresko, P. L. *Nat. Struct. Mol. Biol.* **2016**, *23*, 1092−1100.
(6) Fleming, A. M.; Burrows, C. J. *Chem. Res. Toxicol.* **2013**, *26*, 593−607.
(7) Rhodes, D.; Lipps, H. J. *Nucleic Acids Res.* **2015**, *43*, 8627−8637.
(8) Chen, H.; Long, H.; Cui, X.; Zhou, J.; Xu, M.; Yuan, G. *J. Am. Chem. Soc.* **2014**, *136*, 2583−2591.
(9) Biswas, B.; Kandpal, M.; Vivekanandan, P. *Nucleic Acids Res.* **2017**, *45*, 11268−11280.
(10) Bugaut, A.; Balasubramanian, S. *Nucleic Acids Res.* **2012**, *40*, 4727−41.
(11) Murat, P.; Balasubramanian, S. *Curr. Opin. Genet. Dev.* **2014**, *25*, 22−9.
(12) Miglietta, C.; Cogoi, S.; Marinello, J.; Capranico, G.; Tikhomirov, A. S.; Shchekotikhin, A.; Xodo, L. E. *J. Med. Chem.* **2017**, *60*, 9448−9461.
(13) Gunaratnam, M.; Collie, G. W.; Reszka, A. P.; Todd, A. K.; Parkinson, G. N.; Neidle, S. *Bioorg. Med. Chem.* **2018**, *26*, 2958−2964.
(14) Collie, G. W.; Promontorio, R.; Hampel, S. M.; Micco, M.; Neidle, S.; Parkinson, G. N. *J. Am. Chem. Soc.* **2012**, *134*, 2723−2731.
(15) Perrone, R.; Nadai, M.; Frasson, I.; Poe, J. A.; Butovskaya, E.; Smithgall, T. E.; Palumbo, M.; Palù, G.; Richter, S. N. *J. Med. Chem.* **2013**, *56*, 6521−6530.
(16) Tosoni, E.; Frasson, I.; Scalabrin, M.; Perrone, R.; Butovskaya, E.; Nadai, M.; Palu, G.; Fabris, D.; Richter, S. N. *Nucleic Acids Res.* **2015**, *43*, 8884−97.

(17) Perrone, R.; Nadai, M.; Poe, J. A.; Frasson, I.; Palumbo, M.; Palu, G.; Smithgall, T. E.; Richter, S. N. *PLoS One* **2013**, *8*, No. e73121, DOI: 10.1371/journal.pone.0073121.

(18) Piekna-Przybylska, D.; Sullivan, M. A.; Sharma, G.; Bambara, R. A. *Biochemistry* **2014**, *53*, 2581−93.

(19) Artusi, S.; Nadai, M.; Perrone, R.; Biasolo, M. A.; Palu, G.; Flamand, L.; Calistri, A.; Richter, S. N. *Antiviral Res.* **2015**, *118*, 123−31.

(20) Norseen, J.; Johnson, F. B.; Lieberman, P. M. *J. Virol.* **2009**, *83*, 10336−46.

(21) Murat, P.; Zhong, J.; Lekieffre, L.; Cowieson, N. P.; Clancy, J. L.; Preiss, T.; Balasubramanian, S.; Khanna, R.; Tellam, J. *Nat. Chem. Biol.* **2014**, *10*, 358−64.

(22) Ruggiero, E.; Richter, S. N. *Nucleic Acids Res.* **2018**, *46*, 3270−83.

(23) Henderson, A.; Wu, Y.; Huang, Y. C.; Chavez, E. A.; Platt, J.; Johnson, F. B.; Brosh, R. M., Jr.; Sen, D.; Lansdorp, P. M. *Nucleic Acids Res.* **2014**, *42*, 860−9.

(24) Hanahan, D.; Weinberg, R. A. *Cell* **2011**, *144*, 646−74.

(25) Perrone, R.; Butovskaya, E.; Daelemans, D.; Palu, G.; Pannecouque, C.; Richter, S. N. *J. Antimicrob. Chemother.* **2014**, *69*, 3248−58.

(26) Perrone, R.; Doria, F.; Butovskaya, E.; Frasson, I.; Botti, S.; Scalabrin, M.; Lago, S.; Grande, V.; Nadai, M.; Freccero, M.; Richter, S. N. *J. Med. Chem.* **2015**, *58*, 9639−52.

(27) Yu, Z.; Han, M.; Cowan, J. A. *Angew. Chem., Int. Ed.* **2015**, *54*, 1901−5.

(28) Alagesan, M.; Bhuvanesh, N. S.; Dharmaraj, N. *Eur. J. Med. Chem.* **2014**, *78*, 281−93.

(29) An, Y.; Tong, M. L.; Ji, L. N.; Mao, Z. W. *Dalton Trans.* **2006**, 2066−71.

(30) Jin, Y.; Cowan, J. A. *J. Am. Chem. Soc.* **2005**, *127*, 8408−15.

(31) Liu, J.; Zhang, T.; Lu, T.; Qu, L.; Zhou, H.; Zhang, Q.; Ji, L. *J. Inorg. Biochem.* **2002**, *91*, 269−76.

(32) Qin, X. Y.; Liu, Y. N.; Yu, Q. Q.; Yang, L. C.; Liu, Y.; Zhou, Y. H.; Liu, J. *ChemMedChem* **2014**, *9*, 1665−71.

(33) Doria, F.; Amendola, V.; Grande, V.; Bergamaschi, G.; Freccero, M. *Sens. Actuators, B* **2015**, *212*, 137−144.

(34) Joly, H. A.; Majerus, R.; Westaway, K. C. *Miner. Eng.* **2004**, *17*, 1023−1036.

(35) Huppert, J. L.; Balasubramanian, S. *Nucleic Acids Res.* **2007**, *35*, 406−13.

(36) Doria, F.; Nadai, M.; Folini, M.; Di Antonio, M.; Germani, L.; Percivalle, C.; Sissi, C.; Zaffaroni, N.; Alcaro, S.; Artese, A.; Richter, S. N.; Freccero, M. *Org. Biomol. Chem.* **2012**, *10*, 2798−806.

(37) Hampel, S. M.; Sidibe, A.; Gunaratnam, M.; Riou, J. F.; Neidle, S. *Bioorg. Med. Chem. Lett.* **2010**, *20*, 6459−63.

(38) Micco, M.; Collie, G. W.; Dale, A. G.; Ohnmacht, S. A.; Pazitna, I.; Gunaratnam, M.; Reszka, A. P.; Neidle, S. *J. Med. Chem.* **2013**, *56*, 2959−74.

(39) Valko, M.; Jomova, K.; Rhodes, C. J.; Kuca, K.; Musilek, K. *Arch. Toxicol.* **2016**, *90*, 1−37.

(40) Minotti, G.; Aust, S. D. *J. Biol. Chem.* **1987**, *262*, 1098−104.

(41) Ohyashiki, T.; Nunomura, M.; Katoh, T. *Biochim. Biophys. Acta, Biomembr.* **1999**, *1421*, 131−9.

(42) Aruoma, O. I.; Halliwell, B.; Gajewski, E.; Dizdaroglu, M. *Biochem. J.* **1991**, *273*, 601−4.

(43) Scalabrin, M.; Siu, Y.; Asare-Okai, P. N.; Fabris, D. *J. Am. Soc. Mass Spectrom.* **2014**, *25*, 1136−45.

(44) Meijler, M. M.; Zelenko, O.; Sigman, D. S. *J. Am. Chem. Soc.* **1997**, *119*, 1135−1136.

(45) Pogozelski, W. K.; Tullius, T. D. *Chem. Rev.* **1998**, *98*, 1089−1108.

(46) Brodbelt, J. S. *Annu. Rev. Anal. Chem.* **2010**, *3*, 67−87.

(47) Butovskaya, E.; Heddi, B.; Bakalar, B.; Richter, S. N.; Phan, A. T. *J. Am. Chem. Soc.* **2018**, *140*, 13654−13662, DOI: 10.1021/jacs.8b05332.